Evaluation of ozone column amount from the solar backscattering spectra measured with a spectrograph onboard an aircraft

Toshimi Nakata[1], Kazuyuki Kita[1], Makoto Suzuki[2], Kei Shiomi[3], Shin-ichiro Okumura[4], and Toshihiro Ogawa[3]

[1]*Department of Environmental Sciences, College of Science, Ibaraki University*
[2]*Institute of Space and Astronautical Science, Japan Aerospace Exploration Agency (ISAS/JAXA)*
[3]*Earth Observation Research Center, Japan Aerospace Exploration Agency (EORC/JAXA)*
[4]*Bisei Spaceguard Center, Japan Space Guard Association*

(Received May 7, 2007; Revised July 10, 2007; Accepted July 23, 2007; Online published August 31, 2007)

Slant column amounts of ozone were evaluated from the solar backscattered spectra measured with a simple spectrograph onboard an aircraft over the Pacific Ocean south of Japan in January 2002. A least-squares fitting method optimized on the basis of Bayesian statistics was developed to evaluate them, and the random error in the fitting was about 2.4%. The evaluated slant column amounts of ozone were compared with those calculated from the total ozone data measured with the Total Ozone Mapping Spectrometer (TOMS) on the same day. The differences between the two ranged from a few percent points to more than 20%, and they increased when a small wavelength deviation in the spectrograph occurred due to the aircraft vibration. Excluding the error due to this wavelength deviation, instrumental and systematic errors were estimated to be less than 10%, demonstrating that this airborne measurement with the spectrograph and the developed fitting method could evaluate the ozone column amount with a good accuracy.
Key words: Remote-sensing, ozone, solar ultraviolet spectrum, retrieval, Bayesian statistics.

1. Introduction

The remote sensing of ozone (O_3) column amounts has been conducted mainly by the measurement of the solar ultraviolet (UV) spectra. The total ozone data measured with the Total Ozone Mapping Spectrometer (TOMS) (Heath *et al*., 1975) have been widely used to study and monitor stratospheric O_3. Furthermore, several satellite sensors, such as the Global Ozone Monitoring Experiment (GOME), Scanning Imaging Absorption Spectrometer for Atmospheric Chartography (SCIAMACHY), and the Ozone Monitoring Instrument (OMI), have been utilized for measuring the column amounts of O_3 and other species up to now.

For the validation of satellite remote sensing data, intercomparison with ground-based and aircraft measurements is essential. The airborne remote sensing measurement is effective for the validation of the nadir-looking satellite sensors, because it can provide a series of validation data obtained along the satellite track with a geometry similar to the satellite measurement. It may also provide a good opportunity to estimate the cloud influence on the satellite measurement. For example, Heue *et al*. (2005) measured UV spectra from an aircraft to derive the tropospheric column amount of NO_2 in a wide latitudinal range, and the derived NO_2 column amounts showed a good correlation with those derived from simultaneous SCIAMACHY measurements. However, to date, there have been only a few attempts to validate satellite measurements using airborne remote sensing sensors. Thus, it is significant to develop a remote sensing sensor for airborne measurements and a retrieval algorithm for the sensor data. These can be applied for measuring plumes of air pollution and biomass burning among others. The Airborne Ozone and Pollution measuring UV Spectrometer (Air-OPUS) was developed (Okumura *et al*., 2003) for demonstrating the usefulness of airborne measurements of UV/visible solar back-scattered spectra in estimating amounts of O_3 and atmospheric pollutants such as SO_2 (Watanabe *et al*., 2006) by the Earth Observation Research Center (EORC) at the Japan Aerospace Exploration Agency (JAXA). This study reports the measurements of the solar UV back-scattered spectra by Air-OPUS. A retrieval algorithm to evaluate the O_3 column amounts from the Air-OPUS data has been newly developed. Errors in the measurement and retrieval have been quantitatively estimated to show the performance of this measurement.

2. Instrument

The instrument used in this study, the Air-OPUS, consists of a spectrometer (Jobin-Yvon CP200), a two-dimensional (2-D) CCD camera (PixelVision SV11C), entrance optics, electronics, and a computer to control the measurement and to record the data. The focal length of the spectrometer are 190 mm, and the wavelength resolution is about 0.9 nm. The 2-D CCD consists of 1100 (channels) $\times$ 330 (rows) pixel matrix. The spectra between 190 nm and 455 nm were divided and detected by 791 pixels in the 1100 CCD pixel channels, and the wavelength interval is 0.34 nm. The entrance optics consists of a shatter, a glass, a band-pass (280–370 nm) optical filter, and a quartz lens. Other details about Air-OPUS have been published by Okumura

Table 1. Date, time (in Japanese standard time), location (latitude and longitude, in degree) and SZA (in degree), in which the reference (I_0) and target (I) spectra analyzed in this study were measured.

No	Day	I_0(Reference Spectra)			I(Target spectra)		
		Time	Location	SZA	Time	Location	SZA
1	Jan 10	12:30	27.754, 139.17	50.8	10:45	34.228, 139.20	58.2
2	Jan 10	12:30	27.754, 139,17	50.8	14:00	33.134, 139.42	63.2
3	Jan 10	12:30	27.754, 139.17	50.8	14:30	34.580, 138.58	67.7
4	Jan 13	13:00	34.294, 129.09	56.1	14:30	31.660, 130.10	60.6
5	Jan 19	12:30	22.299, 125.00	42.8	16:00	27.558, 127.81	68.2
6	Jan 20	14:40	29.910, 131.43	59.6	16:30	27.300, 134.72	78.4
7	Jan 21	12:50	23.992, 133.19	44.5	15:00	31.683, 130.76	63.1

et al. (2003) and Watanabe *et al.* (2006). The Air-OPUS was installed onto the bottom of an observation aircraft to measure the spectra backscattered near the surface from the nadir direction. The direction of the entrance slit of the spectrometer was aligned perpendicularly to the flight track, and the spectra backscattered from the directions within 7.5° right and left of the aircraft vertical axis were divided and detected by 330 pixel rows of the CCD.

3. Observation

The Air-OPUS measurement was conducted from 6 to 23 January 2002 during the aircraft observation campaign, Pacific Exploration of Asian Continental Emission (PEACE)-A. The objective of PEACE-A was understanding the characterization of polluted air masses transported over eastern Asia and their chemical transformations (Parrish *et al.*, 2004; Kondo *et al.*, 2004). Sensors for in situ measurement of O_3, CO, NMHCs, NO, NO_y, H_2O, and species were installed on a Gulfstream-II aircraft as well as Air-OPUS. Although in total 13 observational flights were conducted from Nagoya (35.3°N) and Kagoshima (31.6°N) during PEACE-A, the data suitable for the analysis were obtained only in five flights, in which the solar zenith angle (SZA) exceeded about 60°. The observation time, location and SZA in which the data were derived are listed in Table 1. During the flights, each spectrum was obtained at a time interval of 30 sec. In this study, spectra at wavelengths between 315 and 325 nm were analyzed because both the O_3 absorption and the backscattered light intensity are sufficiently large in this wavelength range. To improve the signal-to-noise ratio, the spectrum signals obtained by the ten central pixel rows, which measured the backscattered light nearly along the aircraft vertical axis, were averaged, giving a field of view was about 0.45° across the flight track and 0.045° along it. In addition, the data derived successively in each 10-min period were averaged. The spectrum data significantly affected by high altitude clouds or by the change of aircraft attitude were excluded from the analyses. Thus, the spectrum data obtained during level flights at an altitude between 8 and 11 km were analyzed.

4. Data analysis

The Air-OPUS measured the solar UV spectral intensity backscattered from the nadir direction. Based on Lambert-Beer's law, the measured spectral intensity at a wavelength of λ, $I(\lambda)$ can be approximated as

$$I(\lambda) = sr(\lambda) I_s(\lambda) \exp[-\sigma_{O_3}(\lambda) SC_{O_3}(\chi) - \sigma_R(\lambda) SC_R(\chi) - \sigma_M(\lambda) SC_A(\chi)][F_R(\chi)\sigma_R(\lambda)[M] + F_M(\chi)\sigma_M(\lambda)[A]] \exp[-\sigma_{O_3}(\lambda) VC_{O_3} - \sigma_R(\lambda) VC_R - \sigma_M(\lambda) VC_A] \quad (1)$$

where $sr(\lambda)$ is the spectral sensitivity of the Air-OPUS, $I_s(\lambda)$ is the solar spectral intensity at the top of the atmosphere, $F_R(\chi)$ and $F_M(\chi)$ are the phase functions for the Rayleigh and Mie scattering from the SZA of χ to the zenith direction, respectively, and [M] ([A]) is number density of atmospheric molecules (aerosols) at the scattering altitude, where the backscattering occurred. Because most of the analyzed spectra were obtained over low-level clouds during PEACE-A, the scattering altitude can be considered to be the cloud-top altitude. $\sigma_{O_3}(\lambda)$, $\sigma_R(\lambda)$, and $\sigma_M(\lambda)$ are cross sections of the O_3 absorption, the Rayleigh scattering by atmospheric molecules, and the Mie scattering by aerosols, respectively. $SC_{O_3}(\chi)$, $SC_R(\chi)$, and $SC_A(\chi)$ are the slant column densities of O_3, atmospheric molecules and aerosols between the top of the atmosphere and scattering altitude, respectively. VC_{O_3}, VC_R, and VC_A are their corresponding vertical column densities between the scattering altitude and aircraft altitude. In Eq. (1), multiple scattering before and after the backward-scattering at the scattering altitude was neglected. The absorption by atmospheric molecules except ozone was also neglected. Replacing the sum of SC and VC as SC^*, Eq. (1) can be simplified to be

$$I(\lambda) = sr(\lambda) I_s(\lambda)[F_R(\chi)\sigma_R(\lambda)[M] + F_M(\chi)\sigma_M(\lambda)[A]] \exp[-\sigma_{O_3}(\lambda) SC^*_{O_3}(\chi) - \sigma_R(\lambda) SC^*_R(\chi) - \sigma_M(\lambda) SC^*_A(\chi)] \quad (2)$$

In Eq. (2), $I_s(\lambda)$ could not be measured. Instead, the spectral intensity measured at the time of the smallest SZA, $\chi 0$, during each observation flight was used as the reference spectrum, $I_0(\lambda)$. If the aircraft altitude and scattering altitude for $I(\lambda)$ were similar to those for $I_0(\lambda)$, the ratio of $I(\lambda)/I_0(\lambda)$ was approximately expressed as

$$I(\lambda)/I_0(\lambda) = \exp[-\{\sigma_{O_3}(\lambda)\Delta SC_{O_3} + \sigma_R(\lambda)\Delta SC_R + \sigma_{\mathrm{Ring}}(\lambda)\Delta SC_{\mathrm{Ring}} + Tr(\lambda)\}] \quad (3)$$

where ΔSC_{O_3} (ΔSC_R) is the differential slant column density between $SC^*_{O_3}(\chi)$ and $SC^*_{O_3}(\chi 0)$ ($SC^*_R(\chi)$ and $SC^*_R(\chi 0)$). The ring effect is considered in Eq. (3), and $\sigma_{\mathrm{Ring}}(\lambda)$ and $\Delta SC_{\mathrm{Ring}}$ are the equivalent cross section and the equivalent difference slant column for the ring effect, respectively. We introduced the term, $\exp(-Tr(\lambda))$, to express the product of the terms whose dependence on λ is small, including the Mie scattering terms, $F_R(\chi)\sigma_R(\lambda)$[M], and $sr(\lambda)$. In this study, the $\sigma_{O_3}(\lambda)$ values provided by Bremen University (http://www.iup.physik.uni-bremen.dec/ungruppen/molspec/index.html) were used. Their temperature dependence is compensated by the weighted average of $\sigma_{O_3}(\lambda)$ along the light path. The temperature and O_3 density profiles, measured with ozonesondes by the Japan Meteorological Agency (JMA) at Tateno (36.1°N) in January between 1980 and 1995, were averaged and used for this compensation. The $\sigma_R(\lambda)$ values were calculated using a polynomial equation fitted to those values given by Bates (1984) within a 1% error range. The reciprocal values of $I_0(\lambda)$ were used as the $\sigma_{\mathrm{Ring}}(\lambda)$ values, which are approximately proportional to the incident light intensity (Johnston *et al.*, 1989). A monotonous component of the $\sigma_{\mathrm{Ring}}(\lambda)$ value was removed by subtracting a linear line fitted to the reciprocal values of $I_0(\lambda)$.

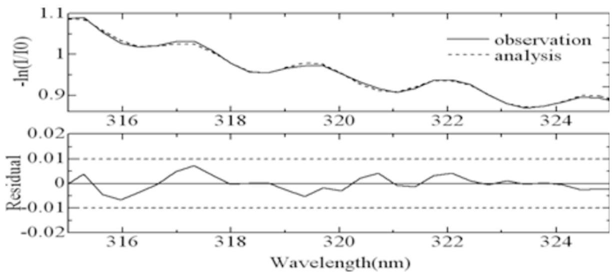

Fig. 1. (Upper panel) Log ratios of I and I_0, derived from the No. 2 measurement on January 10 (solid curve), and calculated from the analysis results (dotted curve). (Lower panel) The residual between the measurement and calculation.

Based on the Bayesian statistics (Higuchi *et al.*, 1989), we evaluated the ΔSC_{O_3} values in Eq. (3) by minimizing the value,

$$|L - (X^t b + dD^t T)| \tag{4}$$

where $L = (ln(I(\lambda_1)/I_0(\lambda_1)), ln(I(\lambda_2)/I_0(\lambda_2)), \ldots, ln(I(\lambda_n)/I_0(\lambda_n)))$ is a vector of the logarithmic ratio of the measured target spectra($I(\lambda)$) and reference spectra ($I_0(\lambda)$), and n is the number of the wavelength division. X is an $n\times(n+3)$ matrix defined by

$$X = \begin{bmatrix} \sigma_{O_3}(\lambda_1), & \sigma_R(\lambda_1), & \sigma_{\text{Ring}}(\lambda_1), & 1, & 0, & \ldots & 0 \\ \sigma_{O_3}(\lambda_2), & \sigma_R(\lambda_2), & \sigma_{\text{Ring}}(\lambda_2), & 0, & 1, & \ldots & 0 \\ \vdots & & & \vdots & & \ddots & \vdots \\ \sigma_{O_3}(\lambda_n), & \sigma_R(\lambda_n), & \sigma_{\text{Ring}}(\lambda_n), & 0, & 0, & \ldots & 1 \end{bmatrix}$$

b and T are vectors defined by $b = (\Delta SC_{O_3}, \Delta SC_R, \Delta SC_{\text{Ring}}, Tr(\lambda_1), Tr(\lambda_2), \ldots, Tr(\lambda_n))$ and $T = (Tr(\lambda_1), Tr(\lambda_2), \ldots, Tr(\lambda_n))$, respectively. ${}^t b$ and ${}^t T$ indicates the transposed vector of b and T. $|.|$ denotes the standard Eulerian norm value. Because the wavelength dependence of $Tr(\lambda)$ is small, the differentiation of it by the wavelength should be small. D is a matrix to calculate the second-order differentiation of the T vector

$$D = \begin{bmatrix} 1, & -1, & 0, & \ldots & \ldots & 0 \\ 1, & -2, & 1, & 0, & \ldots & 0 \\ \vdots & & & \vdots & & \vdots \\ 0, & \ldots & 0, & 1, & -2, & 1 \end{bmatrix}$$

and d is a hyperparameter determining the strength of the restriction, $D^t T = 0$. By minimizing the $|L - (X^t b + dD^t T)|$ value and maximizing the log likelihood (Akaike's Bayesian Information Criterion: ABIC), the d value and b vector, including the ΔSC_{O_3} value, were determined.

5. Results

The upper panel of Fig. 1 compares the $L(\lambda) = -ln(I(\lambda)/I_0(\lambda))$ values measured on January 10 (No. 2 in Table 1) with those calculated from the evaluated values of ΔSC_{O_3}, ΔSC_R, ΔSC_{Ring}, and $Tr(\lambda)$. These two values generally agreed well with each other, and the residual values were mostly less than 1%. Random error in the fitting is estimated to be about 2.4% from the ratio of the root mean square residual values to the difference of the maxima and minima of $\sigma_{O_3}(\lambda)\Delta SC_{O_3}$ values in the 315–325 nm range. In Table 2, the ΔSC_{O_3} values evaluated from the Air-OPUS data were compared with those calculated from the total O_3 values measured with TOMS and those measured with the JMA Dobson spectrometers at Tateno, Kagoshima, and Naha (26.2°N) on the same day. Two total

Table 2. Comparison of the ΔSC_{O_3} values obtained from the Air-OPUS data with those from the TOMS data (∗ denotes that the Dobson data used in the calculation). The absolute and relative values of their difference are represented in DU and percents, respectively.

No	Day	SC_{O3} values(DU)		Difference	
		Air-OPUS	TOMS	(DU)	(%)
1	Jan 10	159.5	146.4	13.1	8.9
2	Jan 10	218.7	212.5	6.2	2.9
3	Jan 10	337.1	358.6	21.5	5.9
4	Jan 13	93.0	57.3	35.7	62.4
			75.0*	18.0*	24.0*
5	Jan 19	228.6	265.0	36.4	13.7
6	Jan 20	513.8	607.4	93.6	15.4
			566.8*	53.0*	9.3*
7	Jan 21	179.4	219.7	40.3	18.3
			215.4*	36.0*	16.7*

O_3 values at the locations where I and I_0 were measured are necessary to calculate the ΔSC_{O_3} values. The TOMS data, given at 1.25° × 1.0 ° grids, at the grid nearest to the measurement locations of $I(\lambda)$ and $I_0(\lambda)$ were used as these values. Considering a large latitudinal difference in the total O_3, the Dobson data could be used as only one of the two values in the three cases when the measurement location of $I(\lambda)$ or $I_0(\lambda)$ was within about 1° in latitude of the Dobson stations. The TOMS data were used as the other value. In these cases, the differences from the calculated ΔSC_{O_3} values from the Dobson and TOMS data were smaller than those only from the TOMS data, suggesting that the Air-OPUS data were more similar to the Dobson data. However, we used the ΔSC_{O_3} values from the TOMS data in the following discussion. The uncertainty of the Earth-Probe TOMS data was evaluated to be 5% in total (McPeters *et al.*, 1998), and the average difference between the Dobson data at the three stations and the TOMS data over them on the 5 days listed in Table 1 was small (−2.3±3.2%). We considered that the data quality of the TOMS data around Japan was enough for the comparison. While the difference between the evaluated ΔSC_{O_3} values and the TOMS values was less than 10% in three cases in January 10, it exceeded 10% in other cases. The difference exceeded 50% in the January 13 case. However, it was due to the small ΔSC_{O_3} value connected with the small difference of SZA, when I_0 and I were measured (see Table 1) in this case. In the other cases, the difference values were not correlated with the ΔSC_{O_3} value, indicating that some systematic errors are significant.

6. Error analysis

During the aircraft observation, a small wavelength deviation, less than the wavelength interval (0.34 nm) of the CCD pixels, in the measured spectra often occurred due to the vibration of aircraft (Watanabe *et al.*, 2006). To show the magnitude of this wavelength deviation, the mean deviation value (δW) was calculated from the ratio between $I(\lambda)$ and $I_0(\lambda)$ to their average at each wavelength

$$\delta W = \sum_{\lambda=340}^{350} [I(\lambda)/I_0(\lambda) - (1/m) \sum_{\lambda=340}^{350} (I(\lambda)/I_0(\lambda))]^2 \tag{5}$$

The δW value was calculated for the wavelength range between 340 and 350 nm, where the O_3 absorption is small, and m is the number of pixels measuring this wavelength range. The δW value increases with the wavelength deviation from $I_0(\lambda)$. $I(\lambda)$ and $I_0(\lambda)$ were the average of each spectrum ($I_i(\lambda)$) derived in a 10-min time interval, and

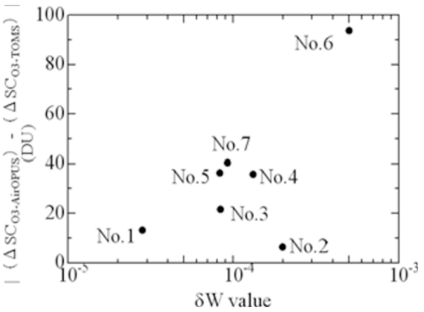

Fig. 2. Scatter plot of the difference between the evaluated ΔSC_{O_3} values and the TOMS ΔSC_{O_3} values versus the δW values. The number in the figure denotes the number of the spectra in Table1 and 2.

spectra with large noises or a large wavelength deviation were excluded from this average by the criterion that the $[I_i(\lambda)/I_0(\lambda) - (1/m)\sum(I_i(\lambda)/I_0(\lambda))]$ value was less than ± 0.0025 at each wavelength. However, the remaining small deviation affects the data quality significantly, because it is equivalent to the increase of the error in $\sigma_{O_3}(\lambda)$ and $\sigma_{Ring}(\lambda)$ and it also increases random errors in $\ln(I/I_0)$. Figure 2 shows a positive correlation of the difference between the evaluated ΔSC_{O_3} values and the TOMS values with the δW values, suggesting that the wavelength deviation caused a dominant error.

Another instrumental error was caused by the uncertainty of the instrument function, namely the spectral response of the spectrometer used in Air-OPUS. The instrument function was estimated from the Hg lamp spectra data measured during the PEACE-A campaign. The total error in the instrument function, including random errors, the wavelength deviation of the spectrometer, and the wavelength dependence of the instrument function, were estimated from the measurement of the spectra of the Hg lamp and Mo, Cu, and Ar hollow-cathode lamps after PEACE-A. The error in the full-width half-maximum (FWHM) of the instrument function was estimated to be less than 0.1 nm. This error causes an uncertainty of 6.0±3.7% in the derived ΔSC_{O_3} values.

Other systematic errors have been estimated. The difference of the assumed profiles of the temperature and O_3 number density from the actual profiles can cause the error in the $\sigma_{O_3}(\lambda)$ values. Based on the variability of their measured profiles, this error is estimated to be less than 1%. Interferences due to the SO_2 and HCHO absorption were negligibly small.

7. Summary

A nadir-looking spectrograph, Air-OPUS, was developed to measure the solar UV back-scattered spectrum from an aircraft. The spectral and time resolution is 0.9 nm and 30 s, respectively. The solar UV back-scattered spectra were measured with Air-OPUS during the PEACE-A campaign in January 2002. Slant column densities of O_3 were evaluated from the measured spectra with a retrieval algorithm developed for this measurement based on the Bayesian statistics.

The spectrum ratios calculated from the retrieval result generally agreed well with the measured ratios, and the random error was estimated to be about 2.4%. The O_3 column densities evaluated from this retrieval were compared with those calculated from the TOMS total ozone data, and their difference ranged from a few percentage points to 50%. The difference is positively correlated with the magnitude of a wavelength deviation in the measured spectra, indicating that the wavelength deviation probably due to the aircraft vibration is the dominant error source. Other systematic errors were also estimated quantitatively. Uncertainty in the spectral resolution (the instrument function) was estimated to be 6.0±3.7%. Uncertainty in the adopted $\sigma_{O_3}(\lambda)$ values, due to the difference between the assumed profiles of the temperature and ozone number density from the actual profiles, was estimated to be less than 1%. These results indicate that the Air-OPUS measurement with the developed retrieval algorithm can evaluate the ozone column density within an error less than 10% when the wavelength shift due to the aircraft vibration is small. This error is comparable with that in the satellite observations and is close enough to discuss the statistical differences between airborne measurement and satellite measurements. This study demonstrates that the measurement of solar UV backscattered spectra with a simple, compact spectrograph, such as Air-OPUS, from an aircraft can be used for the validation of satellite measurements of the O_3 column amount and/or the study of various atmospheric chemistry phenomena.

Acknowledgments. The authors are grateful to the staff of Diamond Air Service for their successful aircraft operation.

References

Bates, D. R., Rayleigh scattering by air, *Planet. Space Sci.*, **32**, 785–790, 1984.

Heue, K.-P., A. Richter, M. Bruns, J. P. Burrows, C. V. Friedeburg, U. Platt, I. Pundt, P. Wang, and T. Wagner, Validation of SCIAMACHY tropospheric NO_2-columns with AMAXDOAS measurements, *Atmos. Chem. Phys.*, **5**, 1039–1051, 2005.

Heath, D. F., A. J. Krueger, H. A. Roeder, B. D. Henderson, The Solar Backscatter Ultraviolet and Total Ozone Mapping Spectrometer (SBUV/TOMS) for NIMBUS G, *Optical Eng.*, **14**, 323–332, 1975.

Higuchi, T., K. Kita, and T. Ogawa, Bayesian statistical inference to remove periodic noise in the optical observations aboard a spacecraft, *Appl. Optics*, **27**, 4514–4519, 1988.

Kondo, Y., K. Nakamura, G. Chen, N. Takegawa, M. Koike, Y. Miyazaki, K. Kita, J. Crawford, M. Ko, D. R. Blake, S. Kawakami, T. Shirai, B. Liley, Y. Wang, and T. Ogawa, Photochemistry of ozone over western Pacific from winter to spring, *J. Geophys. Res.*, **109**, doi:10.1029/2004JD004871, 2004.

Johnston, P. V., and R. L. McKenzie, NO_2 observations at 45S during the decreasing phase of solar cycle 21 from 1980 to 1987, *J. Geophys. Res.*, **94**, 3473–3486, 1989.

McPeters, R. D., P. K. Bhartia, A. J. Krueger, J. R. Herman, C. G. Wellemeyer, C. J. Seftor, G. Jaross, O. Torres, L. Moy, G. Labow, W. Byerly, S. L. Taylor, T. Swissler, and R. P. Cebula, Earth Probe Total Ozone Mapping Spectrometer (TOMS) Data Products User's Guide, *NASA/TP-1998-206895*, 1998.

Okumura S., M. Suzuki, S. Yoshida, T. Sano, M. Watanabe, and T. Ogawa, Design and preliminary performance evaluation of airborne hyperspectral imaging spectrograph Air-OPUS, Proc. of the SPIE, **4897**, 36–43, 2003.

Parrish, D. D., Y. Kondo, O. R. Cooper, C. A. Brock, D. A. Jaffe, M. Trainer, T. Ogawa, G. Hubler, and F. C. Fensenfeld., Intercontinental Transport and Chemical Transformation (ITCT 2K2) and Pacific Exploration of Asian Continental Emission (PEACE) experiments: An overview of the 2002 winter and spring intensives, *J. Geophys. Res.*, **109**, doi:10.1029/2004JD004980, 2004.

Watanabe, M., S. Okumura, M. Suzuki, S. Yoshida, S. Kawakami, T. Sano, K. Shibasaki, S. Hatakeyama, K. Kita, and T. Ogawa, Remote-sensing of Volcanic Sulfur Dioxide by the Aircraft-borne Sensor "Airborne-OPUS"—Algorithm Developments and its Validation Experiment, *J. Remote Sensing Soc. Jpn.*, **26**, 173–185, 2006 (in Japanese).

T. Nakata (e-mail: nd4402h@mcs.ibaraki.ac.jp), K. Kita, M. Suzuki, K. Shiomi, S.-i. Okumura, and T. Ogawa